This is a repository copy of *Spatio-temporal modelling of wave formation in an excitable chemical medium based on a revised FitzHugh-Nagumo model*.

White Rose Research Online URL for this paper:
http://eprints.whiterose.ac.uk/74655/

Monograph:
Zhao, Y., Billings, S.A., Guo, Y. et al. (3 more authors) (2010) Spatio-temporal modelling of wave formation in an excitable chemical medium based on a revised FitzHugh-Nagumo model. Research Report. ACSE Research Report no. 1008 . Automatic Control and Systems Engineering, University of Sheffield

Spatio-Temporal Modelling of Wave Formation in an Excitable Chemical Medium based on a Revised FitzHugh-Nagumo Model

Y. Zhao, S.A. Billings, Y.Guo, D.Coca, L.DeMatos, R.I.Ristic,

Research Report No. 1008

Department of Automatic Control and Systems Engineering
The University of Sheffield
Mappin Street, Sheffield,
S1 3JD, UK

March, 2010

Spatio-Temporal Modelling of Wave Formation in an Excitable Chemical Medium based on a Revised FitzHugh-Nagumo Model

Y.Zhao, S.A.Billings, Y.Guo, D.Coca *, L.DeMatos,R.I.Ristic†

March 8, 2010

Abstract

The wavefront profile and the propagation velocity of waves in an experimentally observed Belousov-Zhabotinskii reaction are analyzed and a revised FitzHumgh-Nagumo(FHN) model of these systems is identified. The ratio between the excitation period and the recovery period, for a solitary wave are studied, and included within the model. Averaged travelling velocities at different spatial positions are shown to be consistent under the same experimental conditions. The relationship between the propagation velocity and the curvature of the wavefront are also studied to deduce the diffusion coefficient in the model, which is a function of the curvature of the wavefront and not a constant. The application of the identified model is demonstrated on real experimental data and validated using multi-step ahead predictions.

1 Introduction

The Belousov-Zhabotinskii(BZ) chemical reaction, is one of the most famous examples of excitable media, and has served as a prototype of nonlinear dynamical spatio-temporal chemical systems because of the remarkable property of exhibiting interesting temporal oscillations and spatial patterns. Many methods based on reaction-diffusion equations such as the Oregonator Model [Field and Noyes, 1974; Chou et al., 2007], Brusselator Model [Glansdorff and Prigogine, 1971], the Gray-Scott Model [Gray and Scott, 1983], and the FitzHugh-Nagumo(FHN) model [FitzHugh, 1955], have been developed to simulate the characteristics of propagating waves using simple models which can produce complex generated patterns. But very few investigations have studied how to determine the parameters of models of excitable media by analyzing real

---

*Department of Automatic Control and System Engineering, University of Sheffield, UK.

†Department of Chemical and Process Engineering, University of Sheffield, UK.

experimental data to generate models which can help to understand the underlying system. This paper aims to seek a revised FHN model, to describe the dynamic behaviours of chemical waves by replacing the Oregonator model commonly used in this field. FHN type models have also been used to model nerve fibers and heart tissue as well as chemical reactions. Two properties of travelling waves, the profile of a steady wave and the velocity of wave propagation, are studied in this paper by sampling experimental data from a real BZ reaction. There are two important relationships which have to be considered for understanding and modelling the travelling velocity. One is the consistent average propagation velocity at different spatial positions. The other is the dependence of the normal velocity of the wavefront curvature, which expresses the correlation between the shape and the propagation velocity of the wavefronts. Based on these developments a new approach is introduced to identify the characteristics of travelling waves using a revised FHN model, the parameters of which are linked back to the investigated physical variables. By utilizing such a model, specific patterns in excitable media can be designed by controlling the model parameters. This also helps in predicting patterns which exist under extreme physical conditions and which may be difficult to reproduce in the laboratory, which could be highly attractive in several applications.

Most studies of spirals waves, which do not appear spontaneously for most concentrations in the BZ reaction, use manual perturbation to create the waves. There was no perturbation inducement in our experiments, which may potentially reduce noise on the travelling velocity, and only circular patters are considered in this study.

2   Theory

Mathematically, reaction-diffusion systems can be expressed by an equation of the form:

$$\frac{\partial u}{\partial t} = f(u) + D\nabla^2 u \tag{1}$$

where $u = u(r,t)$ is the variable, f is the reaction term that describes the dynamics of the system and the last term of equation represents diffusion. From the chemical point of view, Zhabotinskii [Zhabotinskii, 1964] suggested that the BZ reaction consists of two main parts: the autocatalytic oxidation of Ce^{3+} by $HBrO_3$ and the reduction of Ce^{4+} by malonic acid and its bromo-derivatives. Br^- is a strong inhibitor of the autocatalytic oxidation of Ce^{3+} because of its rapid reaction with the autocatalyst, which is presumably $HBrO_2$. Traditionally, the description of the BZ reaction kinetics based on Eq. (1) is reduced to a dimensionless form

[Keener and Tyson, 1986]:

$$\frac{\partial u}{\partial t} = f(u, v) + D_u \nabla^2 u$$
$$\frac{\partial v}{\partial t} = g(u, v) + D_v \nabla^2 v \tag{2}$$

where u is proportional to $HBrO_2$, v is proportional to the oxidized form of the catalyst ferroin, ∇^2 is the Laplacian operator, D_u and D_v are diffusion coefficients, $f(u, v)$ and $g(u, v)$ describe the kinetics of the reaction.

Recently, the FitzHugh-Nagumo equation has became a widely used model for reaction-diffusion systems, and is commonly used to simulate propagating waves in excitable media, such as heart tissue and nerve fibers [Luo and Rudy, 1994; Rubin, 1995]. By removing the diffusion of v and normalizing D_u, the equation is traditionally expressed as

$$\frac{\partial u}{\partial t} = u(a - u)(u - 1) - v + \nabla^2 u$$
$$\frac{\partial v}{\partial t} = bu - \gamma v \tag{3}$$

where $0 < a < 1/2$ and $\gamma \geq 0$.

In this paper, to fully describe the dynamic behaviours of propagation velocity experimentally observed in the experiments described below, the model is modified to the form

$$\frac{\partial u}{\partial t} = u(a - u)(u - 1) - v + \nabla^2 u$$
$$\frac{\partial v}{\partial t} = bu - \gamma v + D_v(k)\nabla^2 v \tag{4}$$

where the constants a, b, γ and a function $D_v(k)$ require to be determined from the experimental data and k denotes curvature of the wavefront.

3   Methods

The chemical processor was prepared in a thin layer at room temperature (usually $25°C \pm 1°C$) and the recipe was adapted from [Winfree, 1972]. Data were acquired by a DSLR camera (Canon 450D) with a resolution 2256×1504 pixels in 24bits true color level. The sample rate was chosen as 0.5 frames per second (fps) automatically controlled by a computer through a USB interface. A typical image represents an area of size $13.9cm \times 9.27cm$, with a resolution of $61.7\mu m/pixel$. Many other researchers normally use an analog CCD camera coupled with a frame-grabber, which only supports 800×600 pixel maximal resolution but a higher sample rate (about $25 - 30$fps) [Forester et al., 1989; Belmonte et al., 1997]. The DSLR camera used in our experiments can provide a much higher spatial resolution and better image quality to achieve more details of the wave profile and this allows the calculation of other properties more accurately, which directly determines the accuracy of the parameters to be identified in the

model. The sample rate is not so important here as the BZ reaction is a relatively slow process. As discussed in [Zhao et al., 2007], the blue component of the image shows the biggest difference for distinguishing the wavefront and background compared with the green and red components. Therefore in this paper, only the blue component was extracted from the raw images to represent the propagating waves. In the reaction, the concentration of cerium ions switch between an oxidized state Ce^{4+} and a reduced state Ce^{3+}, causing the reagent to change its color [Chou et al., 2007]. Hence, the variable v in Eq. (4), which is proportional to the oxidized form of the catalyst ferroin, could be mapped by the value of the blue component.

3.1 Profile of a steady wave

A wave which represents an excursion from a steady state and back to it, will be called a pulse wave and can be excited if a certain threshold perturbation is exceeded. In Figure 1.(a), the phase trajectory denoted by *PT1* is the excursion excited by a large perturbation ($u_0 = 0.2, v_0 = 0$ in Eq. (4)). If the perturbation is not strong enough, for example $u_0 = 0.1, v_0 = 0$, the phase state will go back to the steady state very quickly, as illustrated by the phase trajectory denoted as *PT2*. When u was set as a square pulse (see the initial status of Figure 1.(b)) the wave solution for each variable is shown in Figure 1.(b) and (c), demonstrating how waves travel over time. Notice how the profile of a solitary wave is stabilized as time increases. Figure 2.(a) shows a typical steady solitary wave for v. The range denoted by d_1 represents
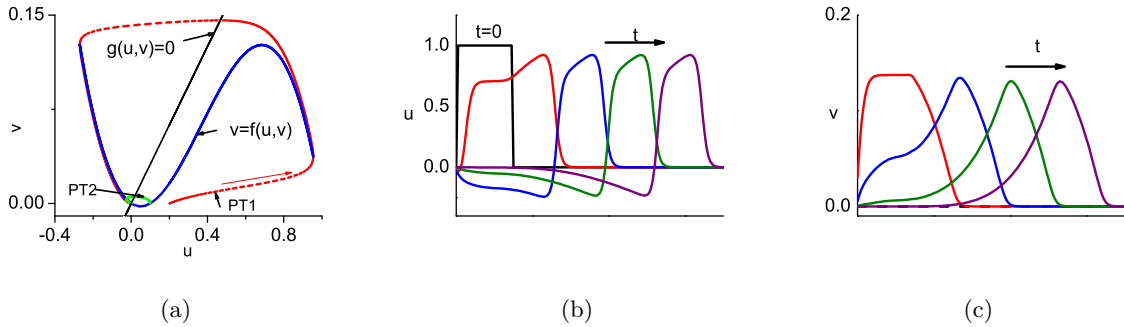

(a)   (b)   (c)

Figure 1: (a) Null clines for FHN with $a = 0.1, b = 0.005, \gamma = 0.0016, D_v = 0$ and phase trajectories for small perturbations ($u_0 = 0.1, v_0 = 0$) and large perturbations ($u_0 = 0.2, v_0 = 0$); (b)-(c)Development of a travelling wave pulse solution from square initial data for Eq. (4) where black denotes initial condition, red, blue, green and purple denote different states over time.

the excitation period and d_2 represents the recovery period. A variable η is introduced in this paper which expresses the ratio of d_1 and d_2

$$\eta = \frac{d_1}{d_2} \tag{5}$$

4

to represent a characteristic of the wave profile. The height and width of the wave are not important here because calibration in space between numerical simulation and experimental data requires further adjustment.

There are four unknown parameters $(a, b, \gamma$ and $D_v)$ in Eq. (4), but it has been found in this study that the value of η only depends on γ. To quantitatively determine this relationship, several simulations with different γ and with the other parameters fixed were implemented and the value of η for each simulation was calculated. The results are shown in Figure 2.(b), where it is observed that the value of η increases following an the increase of γ. Figure 2.(c) shows the sampled data pairs and the corresponding fitted linear model, expressed as

$$\eta = 0.17717 + 17.9482\gamma \tag{6}$$

where $\gamma \geq 0$ or

$$\gamma = -9.8712 \times 10^{-3} + 5.5716 \times 10^{-2}\eta \tag{7}$$

By measuring η from the steady wave profile of the experimental data, parameter γ of a FHN

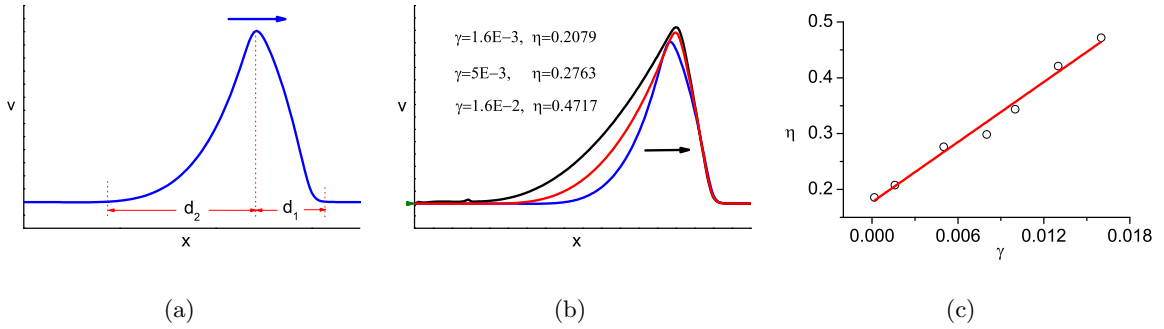(a)   (b)   (c)

Figure 2: (a)A typical steady travelling wave for v;(b)A group of steady travelling waves for v with different γ, where black represents $\gamma = 1.6E - 3$, red denotes $\gamma = 5E - 3$ and blue denotes $\gamma = 1.6E - 2$; (c)Sampled data pairs between γ and η and corresponding fitted linear model.

model can then be approximated by Eq. (7). Ten circular waves in different positions were sampled. The values of η were measured and averaged and the results are

$$\eta = 0.2239$$
$$\gamma = 2.6036 \times 10^{-3} \tag{8}$$

3.2   Propagating velocity of the wavefront

This section discusses the propagating velocity based on experimental data and its dependence on the curvature of the wave boundary. Subsequently, the relationship between the velocity and the diffusion coefficient D_v is investigated to determine D_v based on curvature.

The study starts from the comparison of the averaged propagating velocity of waves in different positions, but which have a similar range of radius. If velocities are not consistent in space, hybrid rules instead of a uniform rule have to be established to fully describe this variable, which can make identification much more complicated. Four circular waves were considered and details of these are given in the first three columns of Table 1, where the units of the second column are in pixels. Velocities of wave propagation were calculated from the time derivative of smoothed radius vs. time. The fourth column of Table 1 shows the averaged propagation

Table 1: Detail of four sampled circles and the corresponding detected velocities.

Symbol	Circle center(x, y)	Sampled frames	Velocity(mm/s)
(a)	970,572	187-223	0.10946
(b)	1600,534	190-224	0.10932
(c)	1230,661	195-230	0.11149
(d)	1030,344	208-232	0.11580

velocity for each pattern, which are all very close. The average velocity of the whole system can then be approximated as $0.1115 \pm 0.0065 mm/s$. The standard deviation is quite small which indicates the system has a consistent average propagating velocity in the space dimension. To verify this conclusion, we also implemented an experiment with exactly the same chemical ingredients, temperature and illumination, but used a high speed digital camera, Phantom V7.0 Colour, to acquire data with a sampling rate of 50fps and image resolution 800×600 pixels. Eight circular waves in different positions were considered to calculate the average velocity and the result was $0.1172 \pm 0.0209 mm/s$. The consistence of the velocity in space certainly seems to exist under our experimental conditions based on high and low imaging. It is also noticed that averaged velocities over both experiments are very close, which suggests that the average propagating velocity may only depend on the chemical ingredients, temperature and illumination.

It has been well proven [Zykov and Morozova, 1980] that the relationship between the normal velocity c and the curvature k of wavefront in a two-dimensional excitable media can be expressed as

$$c = q - D \cdot k \tag{9}$$

where q denotes the velocity of the plane waves, and D is the diffusion coefficient. Experimental evidence has been provided in this paper to confirm this equation. Figure 3 illustrates our

6

experimental results for the relationship between curvature and normal velocity. The data are well represented by a regression line, expressed as:

$$c = 0.1153 - 0.0256 \cdot k \tag{10}$$

where the slope, which corresponds to the diffusion coefficient D, was estimated as $0.0256 mm^2/s$. It is also noticed that the velocity of the plane wavefront makes a large proportional contribution to propagation, which explains why wavefronts visually travel at similar speeds. Values of D and c are not exactly the same as previously obtained in other reports [Forester et al., 1989; Rubin et al., 1997], but are within an acceptable range of difference. It can be explained that both variables are sensitive to illumination and initial concentration of chemical ingredients, and a slight shift in either can significantly change the wave behaviour. Many publications
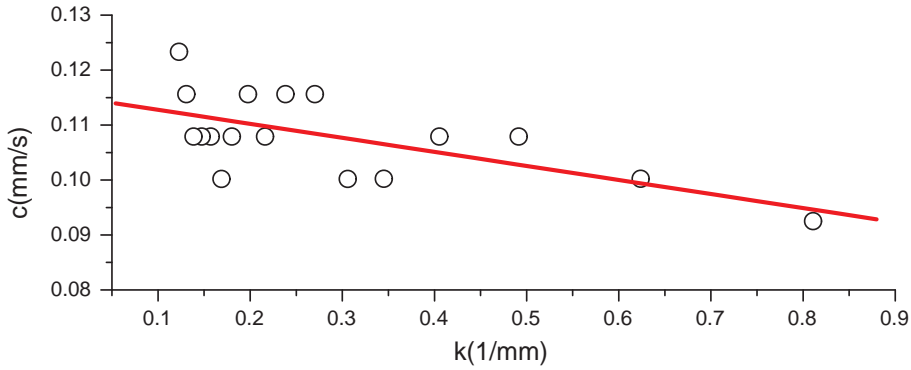

Figure 3: Relation between curvature k and normal velocity c determined from measurements of the dependence of the radius R on the time of outward propagation of circular waves.

on the traditional FHN model have proved that the travelling speed c of a solitary wave in simulation is constant after it enters into steady state. To fully describe the characteristic of c in the BZ reaction which depends on curvature, D_v has to be revised from a constant to a function. Lots of simulations in this paper prove that the travelling velocity of the wavefront c is only dependent on D_v, which indicates D_v can be determined only by curvature k. The relationship between D_v and c was studied by varying the value of D_v from 0 to 1 in simulation, and the results are shown in Figure 4, which clearly demonstrates the relationship is parabolic. The axis for x and y were swopped here because an expression of D_v and curvature k can then be easily obtained if c is located on the horizonal axis. As shown in Figure 4, if D_v is limited in $[0, 1]$, c will be limited in $[0.3544, 0.5188]$. Note the value of c is not important here because
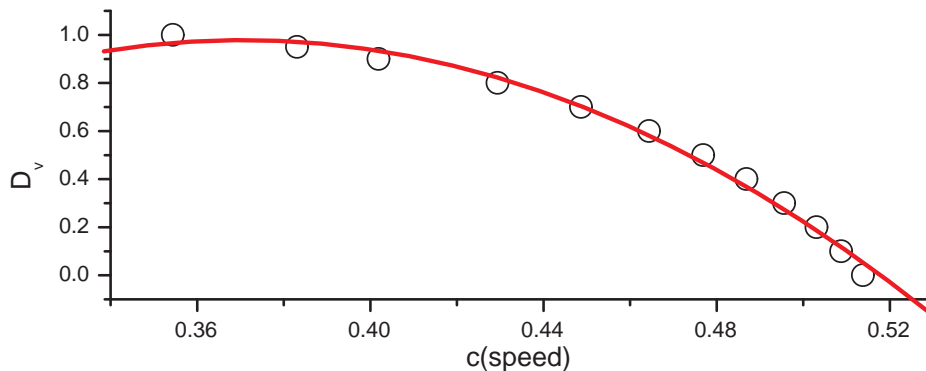
Figure 4: Relationship between travelling speed c and D_v with $a = 0.1, b = 0.005, \gamma = 0.0016$.

it has to be linearly calibrated to physical units later anyway. The ratio of the maximum and minimum of c is 1.46, which covers 1.25, the ratio of the maximum and minimum of c from experimental data. This paper therefor only considers $D_v \in [0, 1]$ as the range is wide enough to fully describe the change of c in our experiments. Of course, if the experimental dish is large enough, the radius of the target pattern could be very big in theory, which means the traveling velocity could be relatively fast based on Eq. (10). However, this paper only aims to describe phenomena shown in our experiments.

Does the selection of D_v affect η that represents the profile of the wavefront? Figure (5).(a) shows three profiles of solitary waves with different choices of D_v. Although the boundary of the waves are not exactly the same, the ratio between the excitation period and the recovery period is close enough, which can be observed more clearly from the normalized waves, shown in Figure (5).(b). Hence, η is independent of D_v, which means that identification of γ and D_v can be considered separately.

3.3 Example based on Real Data

Two sequences of experimental data from the same initial chemical ingredients and environmental conditions were used in this example. The first sequence of data (the estimation set) was sampled to generate a revised FHN model. The second (the testing set) was used to validate the model by comparing the multi-step ahead predictions from the identified model with the data set. The transition rule which describes this system should be consistent if both experiments have the same conditions, and therefore using a testing set, a separate set of data
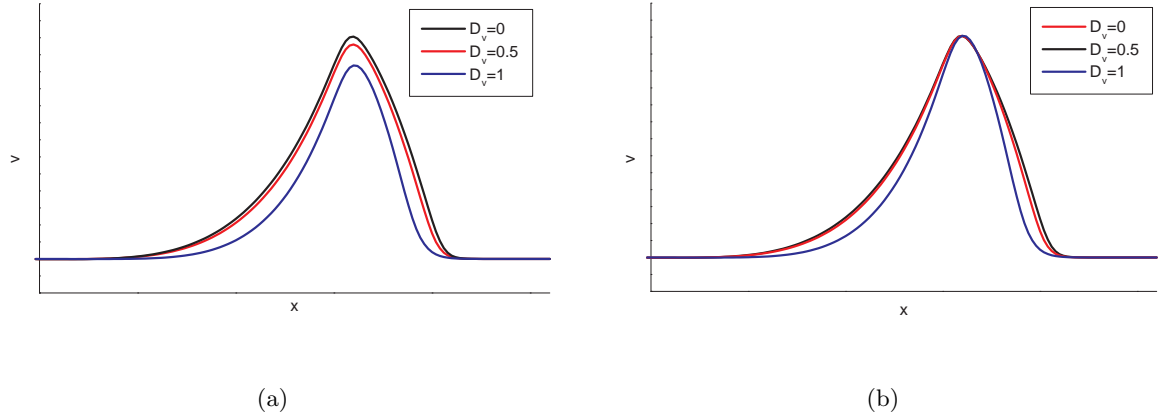
8

(a)

(b)

Figure 5: Comparison of profiles of waves with different values of D_v in the FHN model. (a) original waves; (b) normalized waves

to validate the model, is a good test for model generalisation. The model structure is expressed as Eq. (4), where two critical parameters, γ and D_v, were identified as

$$\begin{aligned}
\gamma &= 2.6036 \times 10^{-3} \\
D_v &= -5.2099 + 133.5932c - 721c^2 \\
c &= 0.1153 - 0.0256 \cdot k
\end{aligned}$$

(11)

Other parameters were set as $a = 0.1$ and $b = 0.005$.

The Euler method was used to discretize derivatives, which are expressed as

$$\begin{aligned}
u(t + \Delta t) &= u(t) + \Delta t \frac{\partial u}{\partial t} \\
v(t + \Delta t) &= v(t) + \Delta t \frac{\partial v}{\partial t}
\end{aligned}$$

(12)

The Lagrange operators ∇^2 were approximated by

$$\nabla^2 u(x,y,t) = \tfrac{1}{4}\Big(u(x+1,y,t) + u(x-1,y,t) + u(x,y+1,t) + u(x,y-1,t)\Big) - u(x,y,t)$$

(13)

where a von-Neumann neighbourhood was used. To evaluate the identified model, the first frame of the second sequence of data was used as the initial condition where the prediction starts. Nearly 50 seconds ahead predictions were produced and five snapshots are shown in Figure 6. Note the excitation of new waves were introduced manually in the prediction. Figure 6 clearly shows visually that the patterns of the predictions are extremely similar to the original experimental captured patterns at each corresponding time. To quantitatively compare the propagating velocity, the radius of three circles from the outside to the inside were measured and are shown in Figure 7.(a). The results in Figure 7.(a) clearly show that the radius at each time are well matched by the prediction. It is also noticed in Figure 7.(b), as expected,
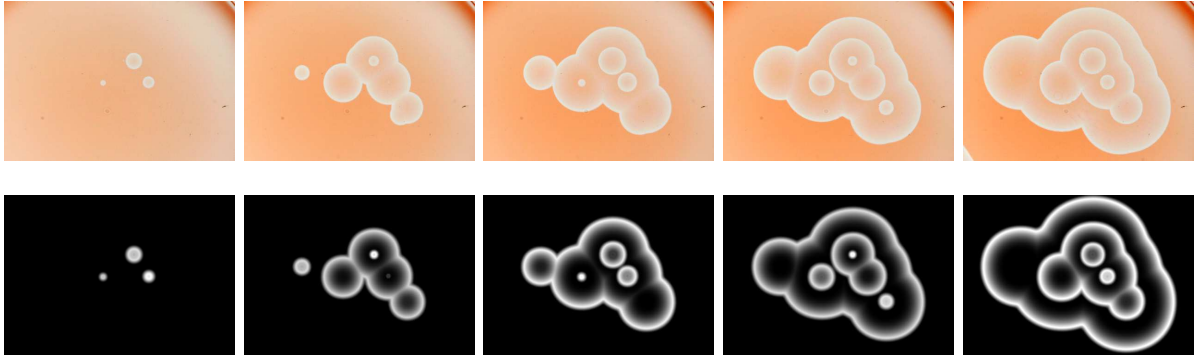
9

Figure 6: Snapshots of the experimental data extracted from the second sequence of experimental data and prediction patterns at corresponding times. The top row shows the original images at time $1s, 20s, 30s, 40s, 50s$; the bottom row shows the predicted patterns at 1 sec (initial condition), plus $19, 19, 39, 49$ seconds ahead.

that the absolute prediction error increases with the time ahead prediction for a certain circle. For multi-step ahead prediction, prediction at the current time depends on prediction at all previous times, and hence the further ahead in time the larger the prediction error will be. Furthermore, slight inconsistency in the rule between the first and second sequence of the data caused by small temperature shifts or ageing of the solution, can also cause prediction errors. The results shown above however strongly suggest that the identified model is a very good representation of wave propagation for real experimental data.
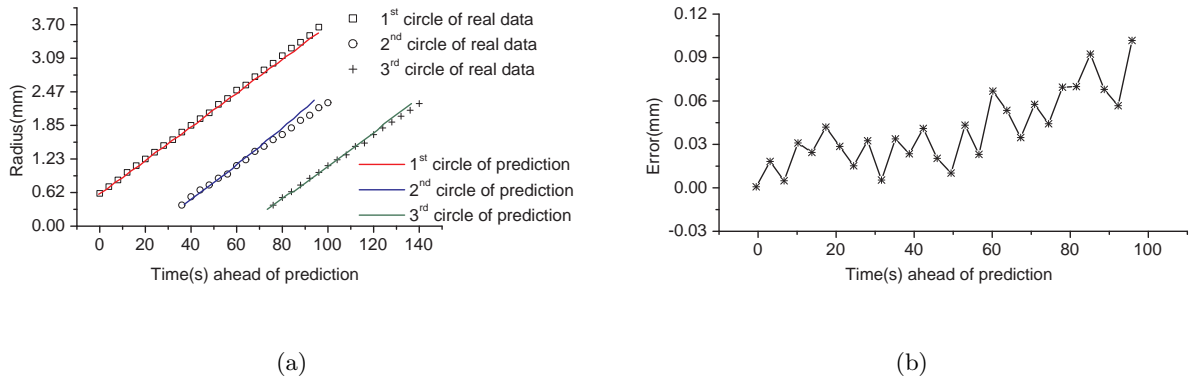

(a)

(b)

Figure 7: (a)Comparison of the radius of three circles over time where the circular points denotes the results from experimental data and the solid coloured lines denote results from model predictions; (b) Illustration of absolute error of prediction for the outside circle.

10

4 Conclusions

The main purpose of this paper was to identify the value of the parameters in a revised FitzHugh-Nagumo model, to describe the dynamic behaviour of propagating waves of BZ reactions. Two properties of the waves, the profile of the wavefront and the propagation velocity, have been discussed. FHN models which have been studied in other publications are usually focused purely on simulations to produce patterns as close to nature as possible. However, this paper solves the inverse problem by estimating the parameters of the model directly from real observed experimental data. The consistency of the average velocity of propagation in different spatial positions has been shown to exist in data sets collected using two kinds of digital camera. This observation supports the approach of using a uniform model to describe wave propagation for all patterns in a sequence of images. Furthermore, the identified parameters are based on physical variables and effects in the model and this, also opens the way to quantitatively establish a relationship between simulations and real systems. It has also been numerically shown that the determination of γ is independent to D_v. An important contribution of this paper, was to show that D_v can be expressed as a function of curvature instead of a constant value which is used in the traditional FHN model. Other parameters assigned typical values to produce steady waves, since they are independent of the characteristics investigated in this paper. The prediction results shown in the example based on real experimental data are highly encouraging. It was observed that the identified model can predict the boundary accurately, even at the 49 seconds (plus 1 sec, initial condition) ahead prediction, which indicates that the identified can represent the dynamic behaviour of circular waves in BZ reactions very well.

Acknowledgment

References

A. L. Belmonte, Q. Ouyang, and Flesselles. J. M. Experimental survey of spiral dynamics in the belousov-zhabotinsky reaction. *Journal de Physique II*, 7:1425–1468, 1997.

M. H. Chou, H. C. Wei, and Y. T. Lin. Oregonator-based simulation of the belousov-

zhabotinskii reaction. *International Journal of Bifurcation and Chaos*, 17(12):4337–4353, 2007.

R. Field and R. Noyes. Oscillations in chemical systems iv. limit cycle behavior in a model of a real chemical reaction. *Journal of Chemical Physics*, 60:1877–1884, 1974.

R FitzHugh. Mathematical models of threshold phonomena in the nerve membrane. *Bulletin of mathematical biology*, 17(4):257–278, 1955.

P. Forester, S. C. Muller, and B. Hess. Critical size and curvature of wave formation in an excitable chemical medium. *Proceedings of the National Academy of Sciences*, 86:6831–6834, 1989.

P. Glansdorff and I. Prigogine. *Thermodynamic Theory of Structure, Stability and Fluctuations*. Wiley Interscience, New York, 1971.

P. Gray and S. K. Scott. Autocatalytic reactions in the isothermal continuous stirred tank reactor: isolas and other forms of multistability. *Chemical Engineering Science*, 38(1):29–43, 1983.

J. P. Keener and J. J. Tyson. Sprial waves in the belousov-zhabtinskii reaction. *Physica D*, 21: 307–324, 1986.

C. Luo and Y. Rudy. A dynamic model of the cardiac ventricular action potential - simulation of ionic currents and concentration changes. *Circulation Research*, 74:1071–1097, 1994.

R. A. Rubin. Heart tissue simulations by means of chemical excitable media. *Chaos, Solitons and Fractals*, 5(3-4), 1995.

R. A. Rubin, Y. Tomohiko, and K. Yoshiki. On the phase dynamics in the bz reaction. *The Journal of Physical Chemistry A*, 101(42), 1997.

A. T. Winfree. Sipral waves of chemical activity. *Science*, 175:634–636, 1972.

A. M. Zhabotinskii. Periodical oxidatation of malonic acid in solution. *Biofizika*, 9:306–311, 1964.

Y. Zhao, S. A. Billings, and A. F. Routh. Identification of the belousov-zhabotinskii reaction using cellular automata models. *International Journal of Bifurcation and Chaos*, 15(5): 1687–1701, 2007.

V.S. Zykov and O.L. Morozova. Speed of spread of excitation in a two-dimensional excitable medium. *Biophysics*, 24:739–744, 1980.